Applied Catalysis B: Environmental 126 (2012) 215–224

Contents lists available at SciVerse ScienceDirect

Applied Catalysis B: Environmental

journal homepage: www.elsevier.com/locate/apcatb

Oxidation of perchloroethylene—Activity and selectivity of Pt, Pd, Rh, and V_2O_5 catalysts supported on Al_2O_3, Al_2O_3–TiO_2 and Al_2O_3–CeO_2. Part 2

Satu Pitkäaho[a,*], Lenka Matejova[b], Kvieta Jiratova[b], Satu Ojala[a], Riitta L. Keiski[a]

[a] University of Oulu, Department of Process and Environmental Engineering, P.O. Box 4300, FI-90014 University of Oulu, Finland
[b] Institute of Chemical Process Fundamentals of the ASCR, v.v.i., Department of Catalysis and Reaction Engineering, Rozvojová 135, 165 02 Prague 6, Czech Republic

ARTICLE INFO

Article history:
Received 16 May 2012
Received in revised form 18 July 2012
Accepted 20 July 2012
Available online 27 July 2012

Keywords:
Catalytic oxidation
Emission abatement
Chlorinated volatile organic compounds (CVOCs)
PCE
Tetrachloroethylene
Reducibility
Acidity
Destructive adsorption

ABSTRACT

Pt, Pd, Rh and V_2O_5 metallic monolith catalysts supported on Al_2O_3, Al_2O_3–CeO_2 and Al_2O_3–TiO_2 were examined in the oxidation of perchloroethylene (PCE). The H_2-TPR experiments proved that the enhanced reducibility is the key feature of the catalyst in PCE oxidation: both the activity and the selectivity followed the orders of catalysts' reducibility. The NH_3-TPD measurements showed that the acidity is not the determining property of the catalyst in the PCE oxidation. After the 40.5 h stability test, no carbonaceous species were seen on the Pt/Al_2O_3–CeO_2 catalyst's surface. Instead, some chlorine was detected on the surface which at this point did not alter the catalysts' performance. During the oxidation strong correlation between the water concentration in the feed and the HCl yield was seen. In the absence of oxygen, i.e. during destructive adsorption, the presence of water had even more pronounced effect on the HCl formation and on the catalysts' stability. The oxidation of PCE over the Pt/Al_2O_3 and Pt/Al_2O_3–CeO_2 catalysts and in the presence of excess hydrogen proceeds via detaching the chlorine atoms before the breakage of the carbon–carbon double bond, and hence following the order of the lowest bond energy in each step.

1. Introduction

The oxidation of unsaturated chlorinated volatile organic compounds (CVOCs) is more difficult than the oxidation of saturated CVOCs. Perchloroethylene (PCE, $Cl_2C{=}CCl_2$) is the most resistant compound among the C_2 chlorinated ethylenes [1–4]. Since there is no hydrogen in the compound itself, a hydrogen source is needed in order to achieve desired selectivity toward HCl [1,5–11]. The above mentioned properties of PCE are setting high demands for the catalyst and oxidation conditions, but also for the materials of experimental set-ups and the treatment facilities. In our previous work [10,12] we confirmed that there exists active and durable catalytic materials among the noble metals for the total oxidation of the CVOCs in an admixture with VOCs. This was concluded since after 23 months of industrial utilization the developed catalysts did not show any significant decrease in the activity. Furthermore, an interesting observation was made during the measurements in industry: the PCE conversions were always higher than that achieved at the laboratory scale. It shows the possible effect of the emission mixture enhancing the PCE conversion, but also the phenomenon that the industrial scale catalytic incinerator operating in transient conditions is highly beneficial in the PCE oxidation [12].

To develop even better catalysts and to understand PCE oxidation more deeply, 15 different samples coated on metallic monoliths were prepared and tested in the first part of this study [11]. But before starting the activity experiments in Ref. [11], the amount of water as a hydrogen source was optimized to 1.5 wt.%. It was shown that the nature of the support affected strongly the activity and selectivity of the catalysts; introduction of TiO_2 and CeO_2 into Al_2O_3 made these supports superior when compared to pure Al_2O_3. From the active phases tested, Pt and Pd showed the highest activity and selectivity and the most active catalyst was the Pt/Al_2O_3–CeO_2 catalyst, having 99% PCE conversion at 690 °C. The activity order of the supports without any active phase was Al_2O_3–CeO_2 > Al_2O_3–TiO_2 > Al_2O_3, and with Pt and V_2O_5 as active phases the order was the same. With Pd and Rh catalysts the activity order of the supports was changed and was now Al_2O_3–TiO_2 > Al_2O_3–CeO_2 > Al_2O_3. Besides higher activity, also higher selectivity toward HCl was seen over the Al_2O_3–CeO_2 and Al_2O_3–TiO_2 supported catalysts. Now the highest HCl yields over the Pt/Al_2O_3–CeO_2 and Pd/Al_2O_3–CeO_2 catalysts reached up to 91% and 93%, respectively. The distribution of the reaction products was studied as well and it was seen that depending on the catalyst, carbon monoxide (CO) and traces of trichloroethylene (TCE, C_2HCl_3), chloroform (TCM, $CHCl_3$) and ethylene (C_2H_4) were formed during

* Corresponding author. Tel.: +358 29448 2374; fax: +358 29448 2304.
E-mail address: satu.pitkaaho@oulu.fi (S. Pitkäaho).

0926-3373/$ – see front matter © 2012 Elsevier B.V. All rights reserved.
http://dx.doi.org/10.1016/j.apcatb.2012.07.025

the light-off tests at the lower temperature range but at higher temperatures only CO, CO_2 and HCl were detected (Cl_2 was not analyzed). More detailed results and discussion can be seen in Ref. [11].

The main objective of this second part of the study was to find out the influence of the reducibility and acidity of these same 15 catalysts on the activity and selectivity in the PCE oxidation. In addition, stability of the Pt/Al_2O_3–CeO_2 catalyst was investigated and tests in N_2 atmosphere (without oxygen) in moist (1.5 wt.% H_2O) and dry conditions were performed in order to evaluate the role of oxygen and water in the PCE reactions. Based on the results, a suggestion of the PCE decomposition over the Pt/Al_2O_3–CeO_2 catalyst is made.

2. Experimental

2.1. Catalysts

The catalysts used were metallic monoliths with the cell density of 500 cpsi prepared by Ecocat Oy. Three different washcoats (Al_2O_3, Al_2O_3–TiO_2 and Al_2O_3–CeO_2) and four different active phases (Pt, Pd, Rh and V_2O_5) were used to prepare all together fifteen samples (12 with active phase). The weight ratio of the Al_2O_3:TiO_2 and Al_2O_3:CeO_2 washcoats was equal to 3:1 and the noble metal loadings were fixed to be equal by the moles and therefore the targeted loadings were 1 wt.% with Pt and 0.5 wt.% with Pd and Rh catalysts. The loading of V_2O_5 was targeted to be 5 wt.%. The final loadings are listed in Table 1. More detailed information about the catalysts and the preparation procedure can be found from Ref. [11].

2.2. Catalyst characterization

If not stated otherwise, the catalyst characterization was performed on the catalysts in their manufactured state, i.e. as metallic monoliths, and in the calculations, only the washcoat was taken into account. The catalysts were characterized by ICP-OES (active metal content), N_2 physisorption at −196 °C (textural properties), CO or H_2 chemisorption (metal dispersions), X-ray diffraction (crystallinity and phase composition), UV–vis diffuse reflectance spectroscopy (vanadium identification), isotopic oxygen exchange (oxygen activation properties) and ion chromatography (chlorine determination). Details of the characterization procedures with the results are given in Ref. [11]. In order to study the properties of the catalysts further NH_3-TPD, H_2-TPR and FESEM-EDS were utilized in this study.

Temperature-programmed desorption (TPD) of NH_3 was carried out to examine acid properties of the catalysts surface. The measurements were accomplished with 0.05 g of powder samples in the temperature range of 20–1000 °C, with helium as the carrier gas and NH_3 as the adsorbing gas. Prior to the measurement, each sample was purged in helium at 500 °C, then cooled to 30 °C and an excess of NH_3 (10 doses, 840 μl) was applied on the sample. After removing physically adsorbed ammonia from the sample by flushing it with helium for 1 h, the heating rate of 20 °C min^{-1} was applied. Omnistar 300 (Pfeiffer Vacuum) mass spectrometer was used to detect the change in the NH_3 concentration. During the experiments the following mass contributions m/z were recorded: 2-H_2, 18-H_2O and 16-NH_3.

Temperature programmed reduction (TPR) measurements were done to 0.2 g powder samples. A mixture of H_2/N_2 (10 mol% H_2) was passed through the sample and the temperature was raised from 20 °C to 1000 °C at a heating rate of 20 °C min^{-1}. A change in the H_2 concentration was detected with a thermal conductivity detector (TCD). Reduction of the grained CuO (0.160–0.315 mm) was performed to calculate the absolute values of hydrogen consumed during the reduction. The TPR and TPD experiments were evaluated using OriginPro 7.5 software with an accuracy of ±5%.

Zeiss Ultra Pluss field emission scanning electron microscope (FESEM) equipped with energy-dispersive X-ray spectroscopy (EDS) at an accelerating voltage of 15.0 kV was used to study the surface of Pt/Al_2O_3–CeO_2 monoliths before and after the 40.5 h stability test and after the tests in N_2 atmosphere. Prior to analysis the samples were coaled to avoid the accumulation of charge. In order to be able to detect the possible coke formation, additional set of samples were pretreated with Pt-sputtering in argon atmosphere resulting in <10 nm Pt-layer on the samples.

2.3. Activity experiments

Catalyst tests were performed in a quartz reactor system described in Ref. [11]. In this study the reaction temperature during the light-off tests ranged from 100 °C to 700 °C (or 500 °C in part of the tests in N_2 atmosphere) and the heating rate used was 10 °C min^{-1}. During the stability test over Pt/Al_2O_3–CeO_2 the oven temperature was set to the T_{90} temperature (600 °C) and the test was performed during one working day in the following way: at the end of the day the gas flow (air + PCE + H_2O) was closed at the same time as the oven was switched off for the night and next morning the gas flow was again turned to the catalyst bed after heating the oven back to 600 °C. The PCE (C_2Cl_4, Algol, 99.0 area%) concentration during all tests was 500 ppm, and if not stated otherwise, to ensure the maximum HCl yield, the activity tests were performed in the presence of 1.5 wt.% water vapour. The flow of the reaction mixture was set to 1.07 l min^{-1} amounting to gas hourly space velocity (GHSV) of 32,000 h^{-1} during all experiments. Depending on the test, compressed air or instrument quality compressed N_2 was used as the carrier gas. Before each test, also a long-term stability test and tests in a N_2 stream, the catalysts were pre-treated. Pre-treatment of the catalysts was always done in an air flow by heating up the catalyst from room temperature (RTP) to 700 °C and then cooling it down to RTP or 100 °C if the test was performed right after the pre-treatment.

The gas analysis during the experiments was done with the Gasmet DX-4000N FTIR analyzer calibrated to detect the following chlorinated hydrocarbons: C_2Cl_4, C_2HCl_3, CH_3Cl, CH_2Cl_2, $CHCl_3$, $COCl_2$ and HCl. Due to the analysis the formation of Cl_2 was not measured and the complete closing of the chlorine-balance was not possible. The selectivity toward HCl, the desired oxidation product, was followed by measuring the HCl concentration at the outlet and calculating the HCl yield, Y_{HCl} [%] as follows: $Y_{HCl} = 100 \times C^{out}_{HCl}/(4 \times C^{in}_{PCE})$ where C^{out}_{HCl} is the measured HCl concentration [ppm], and C^{in}_{PCE} is the feed concentration of PCE [ppm].

3. Results and discussion

3.1. Properties of the catalysts

The total acidity of the catalysts was analyzed by temperature programmed desorption of ammonia (NH_3-TPD) and the total concentration of acid sites between 25 °C and 700 °C was calculated as the amount of ammonia adsorbed per gram of a catalyst (Table 1). Additionally, the strength of the acid sites was determined by considering the strong acid sites being the sites retaining NH_3 at temperatures higher than 300 °C. Accordingly, the sites retaining NH_3 at temperatures lower than 300 °C were considered as the weak acid sites (Table 1). As an example of the TPD profiles observed, the ones of the pure supports are shown in Fig. 1. One main band at the lower temperature range centered at about 140 °C corresponding to the weak acid sites can be seen. However,

Table 1
Metal loading, metal dispersion, acidity and reducibility of the catalysts.

Catalyst	Metal loading (wt.%)	Metal dispersion (%)	Weak acid sites[a] (mmol NH_3 g^{-1})	Strong acid sites[b] (mmol NH_3 g^{-1})	Total acidity[c] (mmol NH_3 g^{-1})	H_2 consumption[c] (mmol $g^{-1}_{catalyst}$)
Al_2O_3	–	–	0.53	0.25	0.78	0.06
Pt/Al_2O_3	0.97	49.4	0.43	0.25	0.68	0.44
Pd/Al_2O_3	0.72	16.2	0.62	0.30	0.92	0.18
Rh/Al_2O_3	0.59	29.0	0.56	0.29	0.85	0.85
V/Al_2O_3	5.7	n.d.	0.60	0.37	0.97	0.47
Al_2O_3–TiO_2	–	–	0.48	0.25	0.73	0.11
Pt/Al_2O_3–TiO_2	1.3	49.8	0.39	0.23	0.62	0.36
Pd/Al_2O_3–TiO_2	0.64	19.5	0.46	0.23	0.69	0.26
Rh/Al_2O_3–TiO_2	0.71	61.0	0.40	0.26	0.66	0.93
V/Al_2O_3–TiO_2	5.2	n.d	0.56	0.36	0.92	0.55
Al_2O_3–CeO_2	–	–	0.52	0.23	0.75	0.31
Pt/Al_2O_3–CeO_2	1.3	35.5	0.42	0.23	0.65	0.70
Pd/Al_2O_3–CeO_2	0.61	32.6	0.50	0.25	0.75	0.47
Rh/Al_2O_3–CeO_2	0.55	74.9	0.50	0.22	0.72	1.13
V/Al_2O_3–CeO_2	5.4	n.d.	0.57	0.27	0.84	0.53

n.d.: not determined.
[a] Temperature range 25–300 °C.
[b] Temperature range 300–700 °C.
[c] Temperature range 25–700 °C.

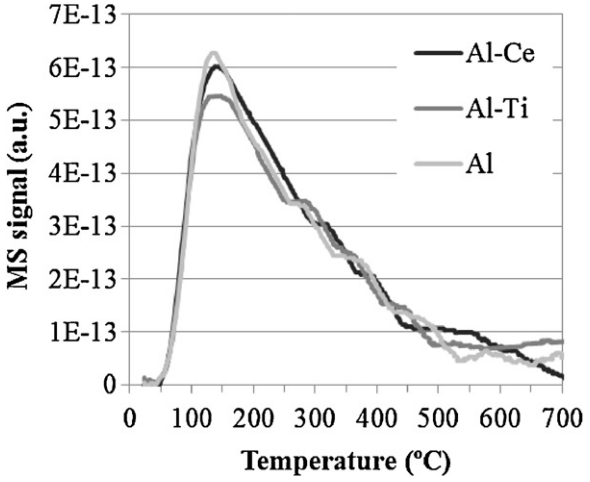

Fig. 1. NH_3-TPD profiles of pure supports.

dispersed TPD profiles from 200 °C to 500 °C evidence the presence of acid sites of different strength – low, medium and strong. For Al_2O_3–CeO_2 and Al_2O_3 there are broad and weak bands centered at 530 °C and 575 °C, respectively, corresponding to a small ratio of strong acid sites. The addition of 23 wt.% of CeO_2 or 26 wt.% of TiO_2 lowered the acidity of the supports (Table 1). When different noble metals added to the supports are compared, the next trend in the total acidity order of the catalysts can be seen: Pd > Rh > Pt, palladium catalysts being the most acidic. In general, the addition of an active phase influenced the acidity the most in the weak sites. When compared to the supports, the acidity was decreased for all the platinum catalysts (Pt/Al_2O_3, Pt/Al_2O_3–TiO_2, Pt/Al_2O_3–CeO_2) and for Pd/Al_2O_3–TiO_2, Rh/Al_2O_3–TiO_2, and Rh/Al_2O_3–CeO_2. Instead, for the Pd/Al_2O_3, Rh/Al_2O_3, V_2O_5/Al_2O_3 and V_2O_5/Al_2O_3–TiO_2 catalysts the total acidity was increased after the addition of the active phase and the contribution to the strong acid sites was notable, indicating increased Brønsted acidity [13]. Over V_2O_5/Al_2O_3–CeO_2 the increase in the total acidity was ~8% belonging mainly to the weak acid sites. Neither the acidity orders of the catalysts nor the strength of the acidity correlated in any way with the oxidation activity orders of these exact catalysts reported in Ref. [11] (see also Table 2) showing that the acid sites are not catalytic active centers for PCE and the acidity is not the determining property of the catalyst in the PCE oxidation.

The reducibility of the different samples was analyzed by temperature programmed reduction experiments with H_2 (H_2-TPR) and the profiles obtained for all the 15 catalysts are shown in Fig. 2a–e. The total hydrogen consumptions of the catalysts between 25 °C and 700 °C are listed in Table 1. For the Al_2O_3-support (Fig. 2a) there are two almost negligible reduction peaks centered at around 110 °C and 495 °C. This is in good agreement with Wu and Kawi [14] who confirmed that hydrogen consumed during TPR reduction of γ-Al_2O_3 is only about 1% of the total theoretical H_2 consumption, indicating that only a small part of γ-Al_2O_3 could be reduced during the H_2-TPR process. The addition of 26 wt.% of TiO_2 to Al_2O_3 shifted these two bands to a slightly lower temperature range, peaks centering now at 90 °C and 430 °C, proposing that the reduction of oxygen on Al_2O_3 is enhanced by the presence of TiO_2. On the Al_2O_3–TiO_2 support the reduction band centered at around 745 °C can be considered to be a reduction of bulk oxygen of TiO_2 [15,16]. The addition of 23 wt.% of CeO_2 to the Al_2O_3 support showed a strong enhancement to the reductive capability of

Table 2
Summary of the activities (temperature at given conversion) and HCl yields at T_{90} temperature of the tested catalysts [11].

	Al_2O_3			Al_2O_3–TiO_2			Al_2O_3–CeO_2		
	T_{50}	T_{90}	HCl yield	T_{50}	T_{90}	HCl yield	T_{50}	T_{90}	HCl yield
–	684	–		660	–		617	–	
Pt	585	–		580	–		492	600	78
Pd	605	–		510	610	84	539	627	83
Rh	560	676	73	522	628	84	540	637	82
V_2O_5 [a]	[b]	–		556	–		520	600	

[a] Over vanadium containing catalysts the light-off test was stopped at 600 °C.
[b] 35% conversion at 597 °C.

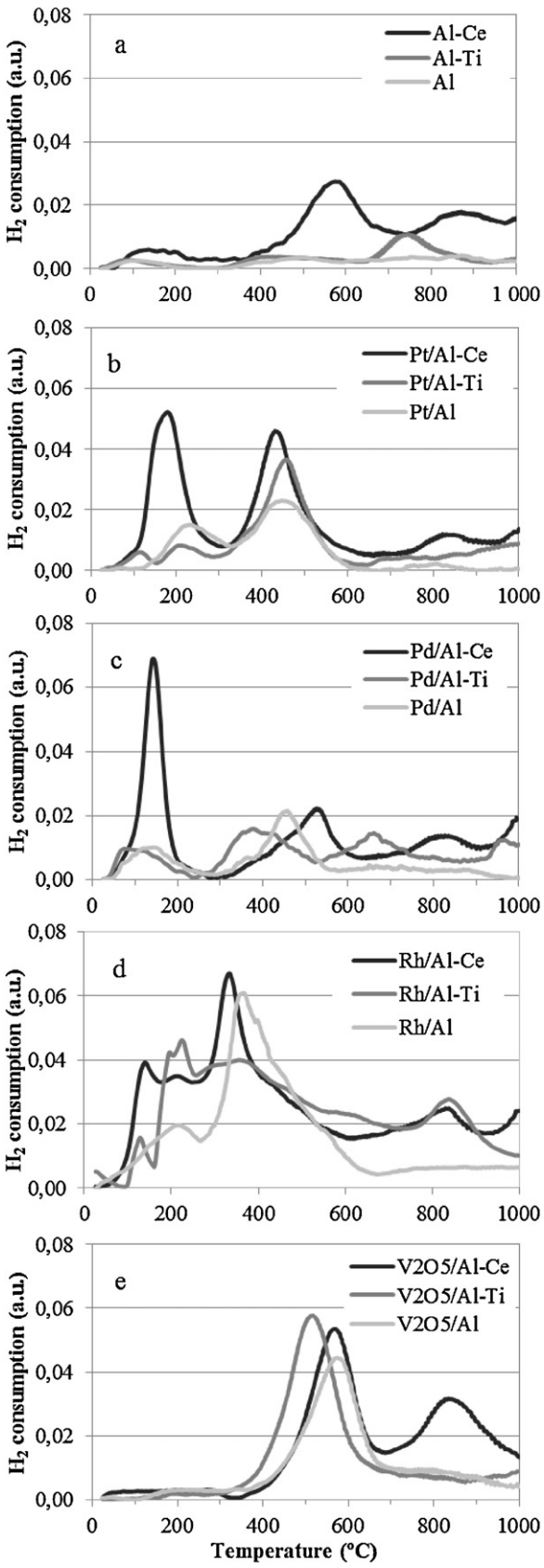

Fig. 2. TPR-H_2 patterns of (a) Al_2O_3, Al_2O_3–TiO_2 and Al_2O_3–CeO_2 supports and all the (b) Pt, (c) Pd, (d) Rh, and (e) V_2O_5 catalysts.

the support as the reduction bands starting from 100 °C have larger peak areas than Al_2O_3 or Al_2O_3–TiO_2 supports (Fig. 2a). Hydrogen consumption is also noticeably higher over the Al_2O_3–CeO_2 support (Table 1). The TPR profile of Al_2O_3–CeO_2 shows all together four peaks: a broad peak centered at 140 °C, a poorly resolved peak at 440 °C as a shoulder which is overlapped with a broad peak with maximum at 570 °C, and a broad peak centered at 860 °C. The peak around 140 °C is probably associated with the reaction of oxygen adsorbed on alumina. The other three peaks can be attributed, respectively, to the removal of surface oxygen from ceria, formation of non-stoichiometric cerium oxides, CeO_x from CeO_2 (x ranging from 1.9 to 1.7) and to the reduction of bulk CeO_2 to Ce_2O_3 [17,18]. The overall reducibility order of the supports without any active phase was Al_2O_3–CeO_2 > Al_2O_3–TiO_2 > Al_2O_3. This is exactly the same order as was reported previously when the activity order of these supports was listed in Ref. [11] (see Table 2) indicating that in PCE oxidation the enhanced reducibility is one of the key properties of the catalyst.

The effect of active phases on the reducibility of the supports can be seen in Fig. 2b–e and Table 1. The addition of a noble metal had only a minor effect on the H_2 consumption in the range of temperatures where bulk reduction of supports take place (T > 700 °C or >600 °C depending on the support), except over Pd/Al_2O_3–TiO_2, which showed an enhanced peak at 660 °C associated with the reduction of bulk oxygen of TiO_2 (Fig. 2c) [15,16,18]. Also over the V_2O_5/Al_2O_3–CeO_2 catalyst some enhancement in the band centered at around 830 °C assigned to the reduction of bulk CeO_2 to Ce_2O_3 or $AlCeO_3$ can be seen (Fig. 2e) [18]. In a lower temperature range (<700 °C), which is the range used during the activity tests, the TPR profiles are clearly modified by the addition of active phases.

The addition of platinum enhanced the reducibility of catalysts over all the supports, especially over Al_2O_3–CeO_2 (Fig. 2b and Table 1). The TPR profile for Pt/Al_2O_3 shows three peaks centered at 70 °C, 230 °C and 450 °C, which could be assigned to the reduction of adsorbed oxygen on alumina, reduction of Pt-oxide species and to the reduction of dispersed Pt on alumina, respectively [18,19]. Besides platinum enhancing the reducibility of the supports, the presence of both titania and ceria on alumina leads to a decrease in the reduction temperature of platinum oxide species, more over the ceria doped than over the titania doped catalyst. This can be seen in Fig. 2b since the reduction peak seen over Pt/Al_2O_3 at 230 °C was now moved to 210 °C with Pt/Al_2O_3–TiO_2 and to 180 °C with Pt/Al_2O_3–CeO_2. The main peak over Pt/Al_2O_3–CeO_2 seen at 180 °C can be considered to result from reduction of Pt but also from the reduction of superficial CeO_2 showing the overall interaction between Pt and ceria. This interpretation is supported by the suppression of the peak seen at 570 °C in Fig. 2a [18,19]. The reducibility of platinum associated with alumina was also increased when titania or ceria was added as is seen from the TPR profiles at around 430–450 °C. However, since with titania the enhancement is not so obvious and because the platinum loading is 1.3 wt.% instead of 0.97 wt.% (see Table 1), the hydrogen consumption enhancement is probably due to higher platinum loading rather than titania. These results are in good agreement with others [15,18–24] and confirm our earlier assumption about the reducibility being one of the determining properties in PCE oxidation [11].

Palladium enhanced the reducibility of all the catalysts as well and once again more with Al_2O_3–CeO_2 than with other supports (Fig. 2c and Table 1). This time the difference in metal loadings cannot explain the enhanced reducibility since the Pd loading on Al_2O_3 was 0.72 wt.% while for Al_2O_3–TiO_2 and Al_2O_3–CeO_2 the loadings were 0.64 wt.% and 0.61 wt.%, respectively. Palladium has been reported to be reduced with H_2 already at room temperature or even below the ambient temperature [25–27], therefore the peaks seen in the TPR profiles in the temperature range

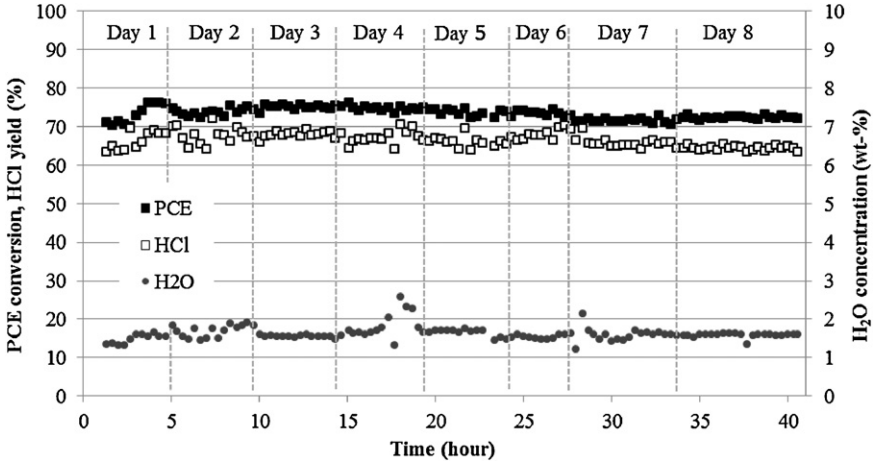

Fig. 3. Stability of $Pt/Al_2O_3–CeO_2$ in the PCE oxidation at 600 °C (PCE 500 ppm, water 1.5 wt.%, GHSV 32,000 h^{-1}).

around 100 °C are probably associated with adsorbed oxygen on the amorphous alumina sites [24]. The addition of Pd enhanced the mobility of oxygen species from the alumina surface with all the catalysts: the TPR profile for Pd/Al_2O_3 shows relatively strong peaks centered at 145 °C and 460 °C with a small shoulder at 360 °C, for $Pd/Al_2O_3–TiO_2$ altogether two reduction peaks in the lower temperature range centered at 80 °C and 380 °C can be seen and for $Pd/Al_2O_3–CeO_2$ the TPR profile shows the strongest peak of all the Pd catalysts at 140 °C. As already mentioned, the third peak centered at 660 °C associated to the reduction of bulk oxygen of TiO_2 [15,16] is now stronger when compared to the support without the active phase. Over $Pd/Al_2O_3–CeO_2$ the additional broad peak at 530 °C with a shoulder at around 390 °C can be assigned to the removal of surface oxygen from ceria and from non-stoichiometric cerium oxides arising during reduction of ceria [18].

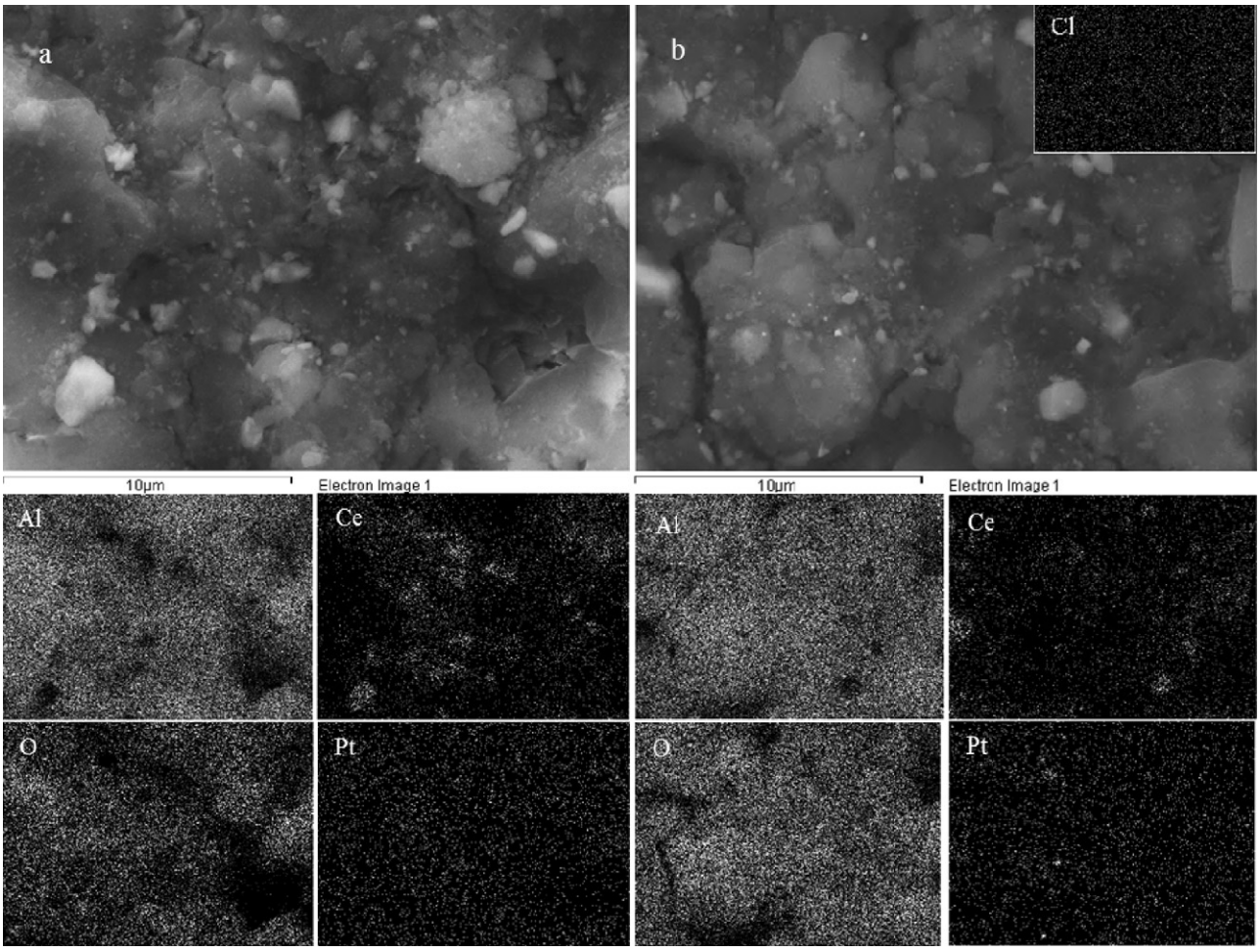

Fig. 4. (a) FESEM image with EDS-mapping of the fresh $Pt/Al_2O_3–CeO_2$ surface and (b) the same catalyst after 40.5 h stability test at 600 °C.

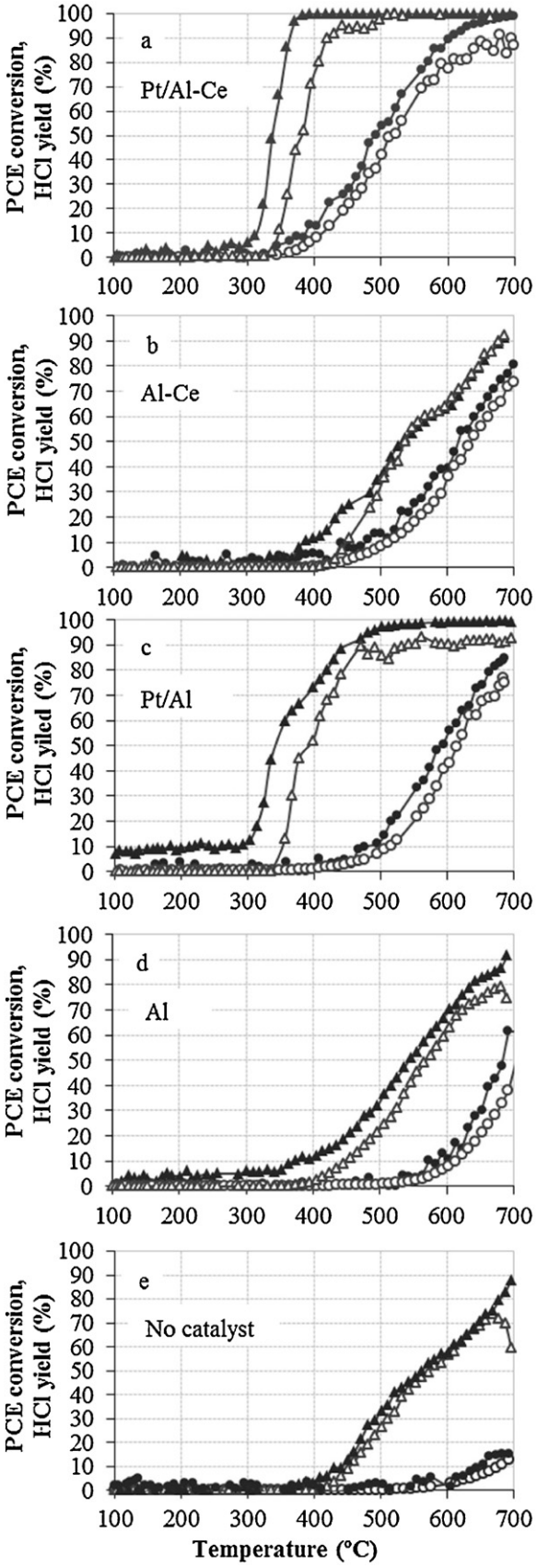

Fig. 5. PCE conversion (filled marker) and HCl yield (empty marker) in N_2 flow and in air flow over (a) $Pt/Al_2O_3–CeO_2$, (b) $Al_2O_3–CeO_2$, (c) Pt/Al_2O_3, (d) Al_2O_3, and (e) an empty reactor (PCE 500 ppm, water 1.5 wt.%, GHSV 32,000 h^{-1}).

The addition of rhodium enhanced the reducibility of all the catalysts, mostly with Al_2O_3 and $Al_2O_3–CeO_2$ but differing from the effect seen with platinum and palladium, the effect was less pronounced with $Al_2O_3–TiO_2$ (Fig. 2d and Table 1). In fact, it could be said that now the addition of TiO_2 to the alumina support inhibited the reducibility of the Rh–catalyst. The TPR profile for Rh/Al_2O_3 showed two overlapping peaks; a broad peak centering at around 215 °C with a weak shoulder at 80 °C and a stronger band with larger peak area centered at 365 °C. Based on the literature [28–34] the first two peaks could be assigned to the reduction of isolated RhO_x species of different size and the third to the reduction of RhO_x species in interaction with the Al_2O_3 support. Four visible TPR peaks for the $Rh/Al_2O_3–TiO_2$ catalyst centering at 120 °C, 218 °C, 350 °C and 830 °C were seen. The first three peaks correspond to the reduction of species seen over Rh/Al_2O_3 (isolated RhO_x and RhO_x interacting with Al_2O_3 support), the fourth peak is assigned to the reduction of bulk oxygen of TiO_2. The week shoulder observed over Rh/Al_2O_3 at 80 °C was now changed to an intense band at 120 °C indicating that there are more small Rh species present [28]. This result is in good agreement with the significantly higher metal dispersion characterized over $Rh/Al_2O_3–TiO_2$; 61% compared to 29% for Rh/Al_2O_3 (Table 1). For $Rh/Al_2O_3–CeO_2$ a similar TPR profile can be seen; four visible reduction peaks centered at 140 °C, 215 °C, 335 °C and 840 °C. The first two peaks can be assigned to the reduction of RhO_x species and the reduction of superficial CeO_2. The third peak corresponds to the reduction of RhO_x species in the interaction with the Al_2O_3 support and the fourth corresponds to reduction of bulk CeO_2 to Ce_2O_3 as seen in all the cerium containing catalysts. The shift to higher temperatures of the first two peaks is correlated with even smaller Rh particles present which is in accordance with the chemisorption showing the highest metal dispersion of ~75% for $Rh/Al_2O–CeO_2$ [28].

Even though vanadium showed rather high overall reducibility (Table 1), the reduction peaks were centered at relatively high temperatures (Fig. 2e), for example for V_2O_5/Al_2O_3 and $V_2O_5/Al_2O_3–CeO_2$ the main peaks were centered at 565 °C and 560 °C, respectively. The TPR peak at 840 °C for $V_2O_5/Al_2O_3–CeO_2$ corresponds again to the reduction of bulk CeO_2 to Ce_2O_3 [18]. For the vanadium on $Al_2O_3–TiO_2$ catalyst the main reduction band was centered now at lower temperature, 505 °C, which can be explained by higher population of tetrahedrally (Td) coordinated vanadium monomers and oligomers observed by the UV–vis DRS in Ref. [11]. Over the Al_2O_3 and $Al_2O_3–CeO_2$ supports higher population of octahedrally (Oh)-coordinated vanadium in 3D polymeric species was detected [11]. Based on the literature [35] the order of reducibility of the vanadium species is the following: Td coordinated monomers ≈ Td coordinated oligomers > Oh coordinated 3D species > V_2O_5.

3.2. Activity and selectivity in PCE oxidation

In the first part of the study [11], the activity and selectivity of all the 15 metallic monoliths, 12 with active phases of Pt, Pd, Rh or V_2O_5 were tested in the PCE oxidation. The activity (T_{50} and T_{90}) and HCl yield at T_{90} of all the 15 catalysts tested is summarized in Table 2. Based on the tests the most active catalyst, $Pt/Al_2O_3–CeO_2$ was chosen for long-term stability tests and for more detailed PCE destruction studies.

3.3. Stability in PCE oxidation

No obvious decrease on the catalysts performance was seen during the 40.5 h stability test for $Pt/Al_2O_3–CeO_2$ in 500 ppm PCE oxidation reaction in moist conditions at 600 °C. The correlation between the water concentration in the feed and HCl yield is obvious as can be seen in Fig. 3: the fluctuation in the water feed affected the HCl yield, higher water content in the gas flow led to

Table 3
Surface area of the $Pt/Al_2O_3–CeO_2$ catalyst as fresh and after the pre-treatment and tests mentioned above.

	Fresh	Pre-treated [a]	After light-off tests[b]	40.5 h in air (H_2O 1.5 wt.%)	~3.7 h in N_2 (H_2O 1.5 wt.%)	~3.7 h in N_2 (no water)
S_{BET} ($m^2\ g^{-1}$)	161	131	97	87	101	90

[a] Pre-treatment in air flow from RTP to 700 °C and back to RTP.
[b] Three light-off tests in air flow (H_2O 1.5 wt.%), pre-treatment between each test.

higher HCl yields and vice versa. FESEM images and EDS-mapping images of the fresh and stability tested $Pt/Al_2O_3–CeO_2$ catalysts are shown in Fig. 4a and b. The EDS-mapping showed that the sharp-edged light particulates are mostly ceria and the darker parts are mostly alumina. It was also seen that the platinum is well dispersed on the catalysts' surface even though the CO chemisorption measurements [11] showed the lowest platinum dispersion for $Pt/Al_2O_3–CeO_2$ catalyst when compared to $Pt/Al_2O_3–TiO_2$ and Pt/Al_2O_3 catalysts (see Table 1). Some visible differences were seen between the images, as after the 40.5 h stability test the catalyst surface looked considerably smoother than the fresh surface. This observation was supported by the fact that after 40.5 h in PCE oxidation the specific surface area (S_{BET}) dropped by ~44 $m^2\ g^{-1}$, from 131 $m^2\ g^{-1}$ to 87 $m^2\ g^{-1}$ (Table 3). Another difference seen was that after 40.5 h, some chlorine was detected on the catalyst surface (Fig. 4b). In our previous study [11] IC measurements showed water soluble chlorine from 2.7 mg g^{-1} to 4.9 mg g^{-1} on the catalysts after 2–4 light-off tests (duration 2–4 h). The chlorine on the surface did not affect the catalysts performance since the $Pt/Al_2O_3–CeO_2$ catalysts did not lose its activity or selectivity after 40.5 h in the PCE oxidation (Fig. 3). One possibility is that chlorine seen on the catalyst surface is chlorine atoms or chloride ions coming from PCE and their removal from the surface as HCl is still unfinished [1,2]. The assumption made in Ref. [11] on insignificant coke formation was confirmed as the FESEM-EDS analysis of the samples pre-treated with Pt-sputtering showed no detectable carbon on the $Pt/Al_2O_3–CeO_2$ catalyst's surface after 40.5 h.

3.4. Reactive adsorption

In order to study the role of water and oxygen in the PCE destruction, light-off tests in the absence of air with Al_2O_3, $Al_2O_3–CeO_2$, Pt/Al_2O_3, $Pt/Al_2O_3–CeO_2$ and with the empty reactor were carried out. One test over $Pt/Al_2O_3–CeO_2$ was also done in dry conditions. The comparison between the light-off tests in N_2 and air atmosphere is shown in Fig. 5a–e. In all the cases the removal of oxygen from the gas stream enhanced the PCE conversion. Over the $Pt/Al_2O_3–CeO_2$ catalyst (Fig. 5a) the removal of oxygen from the gas stream lowered the T_{50} temperature by 150 °C and 90% conversion was now reached already at 365 °C instead of 600 °C. Furthermore, the HCl selectivity was improved and the maximum HCl yield was raised from ~90% to 100%. Above 400 °C the only reaction products detected were CO, CO_2 and HCl. When the same test was performed with the $Al_2O_3–CeO_2$ support (Fig. 5b), the promoting effect coming from the air removal was still seen, but it was weaker than when Pt was present. Over Pt/Al_2O_3 and Al_2O_3 (Fig. 5c and d) similar results were obtained as the enhancement when platinum present was more pronounced. The tests performed with the empty reactor (Fig. 5e) showed that elevated PCE destruction occurred even without a catalyst: PCE destruction started at 410 °C and reached 88% conversion at 700 °C. During the thermal oxidation (in air) the PCE conversion was only minor reaching 15% at 700 °C. The difference in activity between an empty reactor (Fig. 5e) and the tested supports (Fig. 5b and d) was small – indicating that oxygen free atmosphere together with active phase, now platinum is the driving force for enhanced PCE destruction. The difference seen in the removal of PCE in the absence and presence of oxygen suggest that oxygen competes with PCE for the catalysts' surface sites. This has been seen previously also by others [36,37].

The presence of water did not alter the PCE removal efficiency, but to the HCl yield it had a major effect (Fig. 6a); the hydrogen coming from water participates in the formation of HCl preventing the accumulation of unwanted chlorine on the catalyst's surface and therefore inhibits the deactivation.

One very interesting observation came across during these oxygen free tests as the light-off test was always repeated once with the same catalysts after the pre-treatment procedure (explained in Section 2.3) to verify the obtained result. When a noble metal was present, the second conversion curve preserved its shape but the curve was always lifted to the higher temperature region (Fig. 6b). According to Heck and Farrauto [38] this suggests that deactivation of the catalyst happened via a loss of active sites, e.g. sintering. Over the two supports tested in this study (Fig. 6b) and during the PCE oxidation tests of this study as well as in Ref. [11], this kind of rapid deactivation was not seen. To examine the observed deactivation, the light-off test (10 °C min^{-1} from 100 °C to 500 °C) continued with 135 min stability test at 500 °C followed by pre-treatment in air and a second light-off test from 100 °C to 500 °C was performed in N_2 atmosphere over the $Pt/Al_2O_3–CeO_2$ catalyst. Test was performed in dry and in moist conditions and altogether one catalyst was ~220 min in the PCE flow. The results are shown in Figs. 7a–c and 8a–c. During the first light-off test with the fresh catalysts the presence or absence of water did not cause a big difference in the PCE conversion in the lower temperature region (Figs. 7a and 8a), the T_{50} temperature was even a little bit lower in dry conditions than in moist conditions as it was now 350 °C and 355 °C, respectively. At the higher temperature range the removal of water had, however, a major effect, since the maximum HCl yield dropped from 96% to 42% at 500 °C. During the stability test (Figs. 7b and 8b) the difference was more obvious as in dry conditions both the PCE conversion and the HCl yield started to decline and the second light-off test (Fig. 8c) showed that the catalyst did not recover after the pre-treatment procedure in air flow as the activity and selectivity remained low. According to Heck and Farrauto [38] the conversion curve in Fig. 8c indicates both a loss of active sites and masking (covered surface sites or blocked pores). To examine the catalyst surface, FESEM and EDS-mapping images of the tested $Pt/Al_2O_3–CeO_2$ catalyst are shown in Fig. 9a and b. From these figures it is obvious that the chlorine amount on the catalysts' surface is now increased and chlorine is dispersed all over the washcoat, being present on both alumina and ceria. At the same time the oxygen density is lower (Fig. 9b), especially on the clusters where the cerium content is high indicating that ceria has lost some of its oxygen. The EDS-mapping showed also that already after ~220 min in the PCE stream some sintering of the catalysts surface occurred during the oxygen free tests as the cerium clusters grew bigger.

This reaction with an oxygen storage catalyst and absence of oxygen in the gas flow destroying e.g. the PCE and completely converting it to CO_2 is called the reactive adsorption or destructive adsorption process [39–43]. Rupp et al. [42] studied reactive adsorption of PCE on Pt/Rh three way catalysts (TWC) and reported that the presence of O_2 in the reaction gas stream inhibited the reactive adsorption, leading instead to the catalytic oxidation at sufficiently higher temperatures. They also reported that the initially high conversion during this reactive adsorption process is

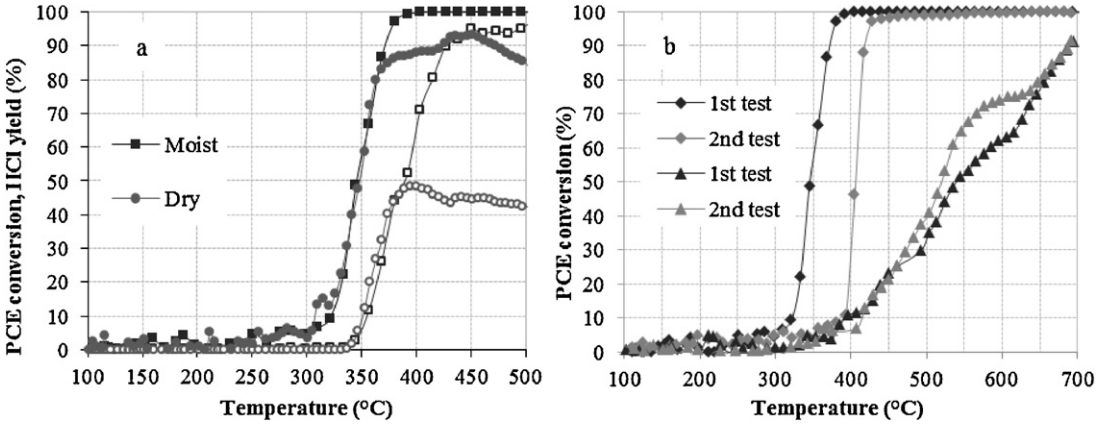

Fig. 6. (a) PCE conversion (filled marker) and HCl yield (empty marker) over $Pt/Al_2O_3–CeO_2$ in moist and dry conditions and (b) PCE conversion over $Pt/Al_2O_3–CeO_2$ and $Al_2O_3–CeO_2$ in moist conditions (water 1.5 wt.%) (PCE 500 ppm, N_2 atmosphere, GHSV 32,000 h^{-1}).

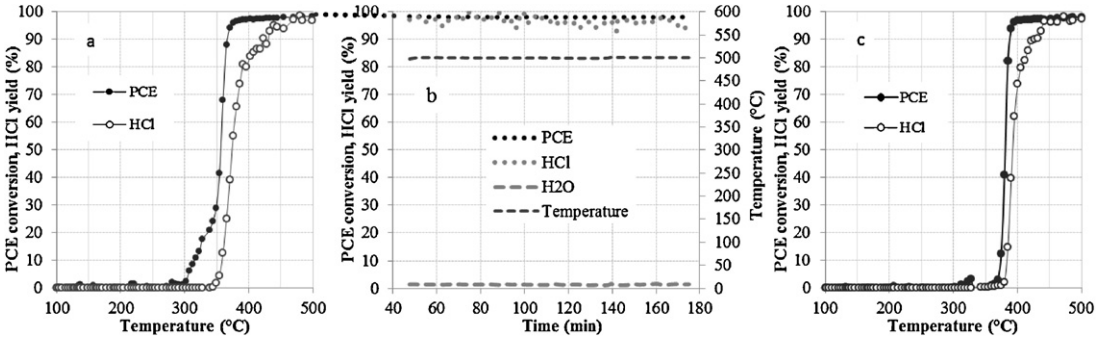

Fig. 7. PCE conversion and HCl yield over $Pt/Al_2O_3–CeO_2$ in moist conditions: (a) light-off test with a fresh catalyst followed by (b) 135 min stability test and (c) light-off test after the stability test. Altogether the catalyst was ~220 min in the PCE flow (the same conditions as in Fig. 6).

only momentary as the conversion drops to 10% within the first hour since the reduction of ceria and the replacement of lattice oxygen with chlorine atoms occurred. To turn this destructive process toward catalytic reaction cycle, a simultaneous de-chlorination, e.g. steaming of the solids is needed. The presence of water vapor has been seen to re-oxidize e.g. the lanthanum oxide to allow the reactive adsorption process to continue indefinitely [43]. In this study, it was seen that in N_2 atmosphere the presence of water inhibited the catalysts deactivation when compared to dry conditions but still some, maybe even quite permanent changes such as sintering was seen on the catalysts surface.

3.5. PCE decomposition over the $Pt/Al_2O_3–CeO_2$ catalyst

To examine the possible by-product formation in more detail, one light-off test with a lower heating rate (now 5 °C min^{-1} instead of 10 °C min^{-1}) and with more frequent data collecting (now every 30 s instead of every 1 min) was done over the $Pt/Al_2O_3–CeO_2$ catalyst. Yet no extra information was gained. As already reported in Ref. [11], the only chlorinated by-product detected was trichloroethylene (TCE, C_2HCl_3), and above 420 °C it was not detected anymore. To understand the role of alumina, ceria and platinum in the PCE oxidation, detected by- and end-products of the thermal experiment as well as for experiment with the Al_2O_3 and $Al_2O_3–CeO_2$ supports together with the Pt/Al_2O_3 and $Pt/Al_2O_3–CeO_2$ catalysts are shown in Table 4. Based on the by-products TCE and ethylene, even though detected in very low quantities, the PCE oxidation over the Pt/Al_2O_3 and $Pt/Al_2O_3–CeO_2$ catalysts in excess hydrogen can be assumed to proceed via the breakage of all chlorides from the carbons before the breakage of double bond between two carbons takes place. Therefore, the PCE

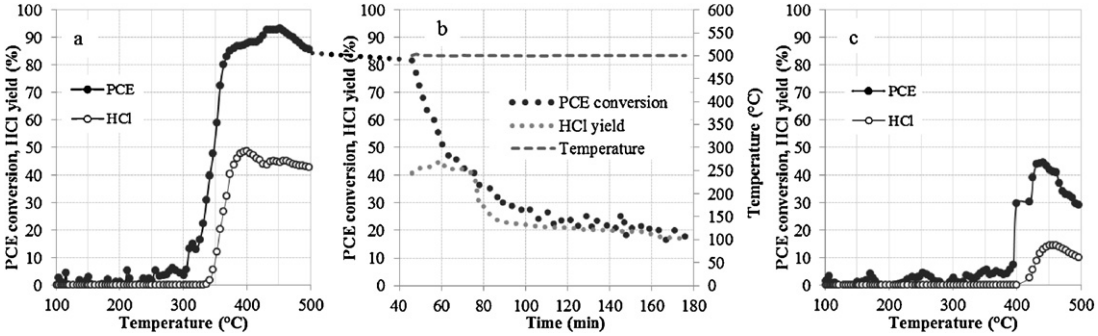

Fig. 8. PCE conversion over $Pt/Al_2O_3–CeO_2$ in dry conditions: (a) light-off test with a fresh catalyst followed by (b) 135 min stability test and (c) light-off test after the stability test. Altogether the catalyst was ~220 min in the PCE flow (the same conditions as in Fig. 6).

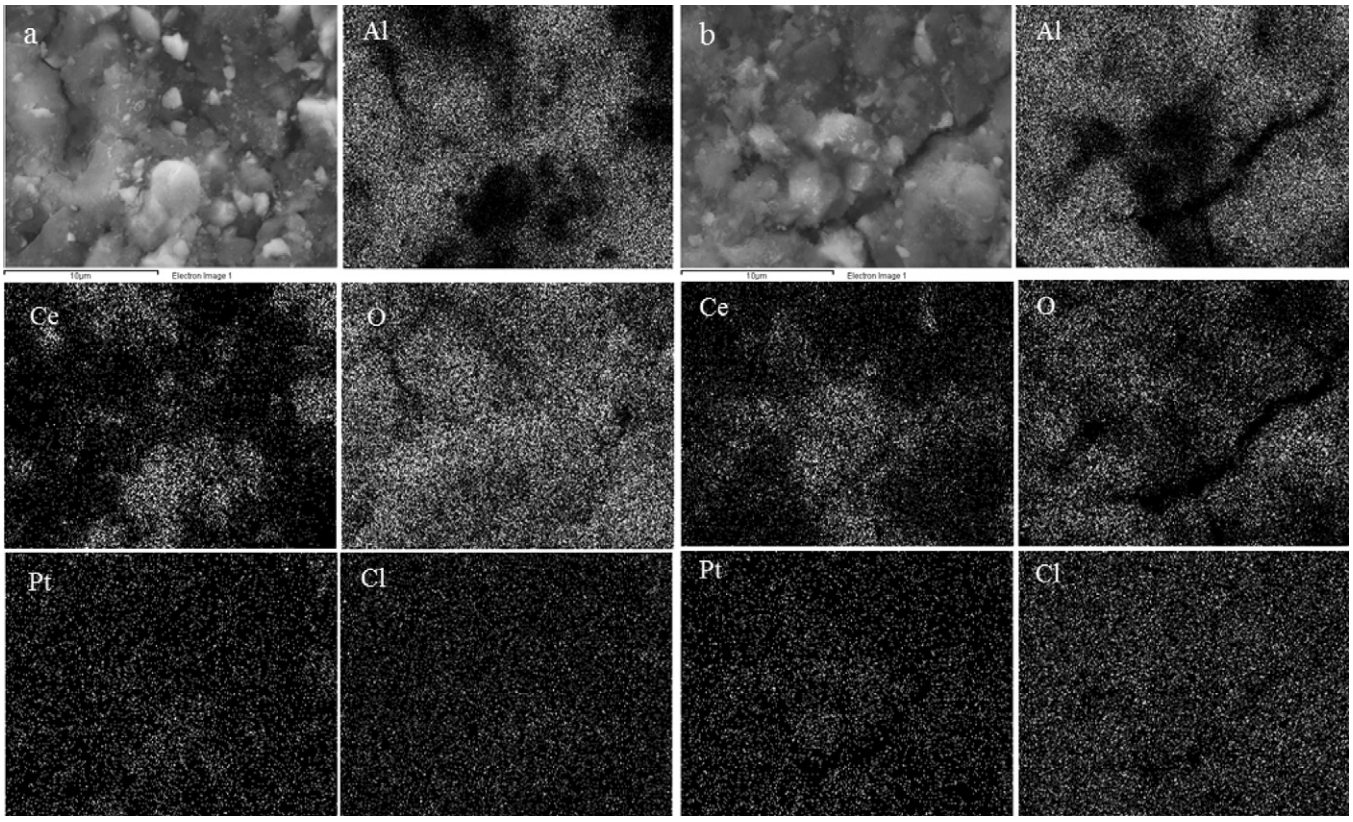

Fig. 9. FESEM image and EDS-mapping of the $Pt/Al_2O_3–CeO_2$ surface after ~220 min in the PCE flow (a) in moist conditions (water 1.5 wt.%) and (b) in dry conditions (the same conditions as in Fig. 6).

Table 4
The side- and end-products detected during the light-off test (temperature from 100 °C to 700 °C, heating rate 10 °C min^{-1}; PCE 500 ppm; water 1.5 wt.% and GHSV 32,000 h^{-1}).

	PCE conv. at 700 °C (%)	TCE[a] (ppm at temp. range, °C)	C_2H_4 (ppm at temp. range, °C)	CO (ppm at temp. range, °C)	CO_2[b] (ppm at temp. range, °C)	HCl (ppm at temp. range, °C)
–	15	–	–	1–23 at 410–700	100–200 at 610–700	5–255 at 480–700
Al_2O_3	62	–	2–12 at 490–630	1–136 at 280–700	100–400 at 445–700	5–1015 at 290–700
$Al_2O_3–CeO_2$	80	–	–	1–165 at 100–700	100–800 at 350–700	5–1580 at 370–700
Pt/Al_2O_3	85	1–4 at 160–400	3–9 at 450–610	1–8 at 100–700	100–1100 at 210–700	9–1570 at 100–700
$Pt/Al_2O_3–CeO_2$	99	1–7 at 100–400	1–9 at 420–470	–	100–1200 at 100–700	8–1800 at 100–700

[a] Trichloroethylene (C_2HCl_3).
[b] CO_2 measurement was done by vol.% and therefore the detection limit is so coarse.

decomposition in each step follows the order of the lowest bond energy calculated at room temperature with the HSC Chemistry Software and reported in Ref. [11].

4. Conclusions

In the first part of this study [11], altogether 15 catalysts were examined in the oxidation of PCE. $Pt/Al_2O_3–CeO_2$ was found to be the most active and selective catalyst among the Al_2O_3, $Al_2O_3–CeO_2$, $Al_2O_3–TiO_2$ supported Pt, Pd, Rh and V_2O_5-catalysts. In this second part of the study the same catalysts were tested and characterized further and the following results are withdrawn:

- The NH_3-TPD acidity tests showed that the addition of an active phase influenced the most the acidity related to the weak acid sites. Depending on the active phase, the impact was positive or negative but the total acidity did not correlate with the oxidation activity of the catalysts showing that the acidity is inconclusive property of the catalyst in the PCE oxidation.
- The H_2-TPR experiments showed that the overall reducibility order of the supports without any active phase was $Al_2O_3–CeO_2 > Al_2O_3–TiO_2 > Al_2O_3$. This is exactly the same order as the activity order of these supports indicating that the enhanced reducibility is one of the key properties over the catalyst in the PCE oxidation. As the activity of oxygen [11] and the redox properties of the catalysts are increased by adding ceria and platinum to the catalyst, not only the PCE conversion is enhanced but also the selectivity toward CO_2 and HCl is improved. Over the $Pt/Al_2O_3–CeO_2$ catalyst, the HCl yield reached 91%, the formation of CO was no longer seen during the light-off test and the formation of CO_2 was further enhanced.
- The 40.5 h stability test for $Pt/Al_2O_3–CeO_2$ in 500 ppm PCE oxidation in moist conditions was carried out at 600 °C and no obvious change in the catalysts performance was seen. No carbonaceous

species was seen on the $Pt/Al_2O_3–CeO_2$ catalyst's surface but instead, some chlorine was detected that at this point did not affect the catalysts' activity or selectivity.

- During oxidation an obvious correlation between the water feed and the HCl yield was seen but to the PCE conversion the change in the amount of water did not have influence. In the absence of oxygen, as the destructive adsorption occurred, the presence of water did not alter the initial PCE removal efficiency but to the HCl formation and to the catalysts' stability it had a major effect.
- The PCE decomposition over the Pt/Al_2O_3 and $Pt/Al_2O_3–CeO_2$ catalysts during the oxidation and in the presence of an additional hydrogen source proceeds via detaching the chlorine atoms before the breakage of the carbon–carbon double bond, hence following the order of the lowest bond energy in each step.

Acknowledgements

This work was carried out with the financial support of the Council of Oulu region from European Regional Development Fund (A30505, OLH-2007-02428/Ha-7) and the City of Oulu. Mr. Jorma Penttinen and Mr. Tuomas Nevanperä are acknowledged for their contribution to the experimental work.

References

[1] G.C. Bond, N. Sadeghi, Journal of Applied Chemistry and Biotechnology 25 (1975) 241–248.
[2] H. Windawi, M. Wyatt, Platinum Metals Review 37 (1993) 186–193.
[3] H. Windawi, Z.C. Zhang, Catalysis Today 30 (1996) 99–105.
[4] P.S. Chintawar, H.W. Greene, Applied Catalysis B (1997) 81–92.
[5] G. Sinquin, C. Petit, S. Libs, J.P. Hindermann, A. Kiennemann, Applied Catalysis B 27 (2000) 105–115.
[6] J.R. González-Velasco, A. Aranzabal, R. López-Fonseca, R. Ferret, J.A. González-Marcos, Applied Catalysis B 24 (2000) 33–43.
[7] R. López-Fonseca, S. Cibrián, J.I. Gutiérrez-Ortiz, M.-A. Gutiérrez-Ortiz, J.R. González-Velasco, AIChE Journal 49 (2) (2003) 496–504.
[8] K. Everaert, J. Baeyens, Journal of Hazardous materials B109 (2004) 113–139.
[9] R. López-Fonseca, J.I. Gutiérrez-Ortiz, J.R. González-Velasco, Catalysis Communications 5 (2004) 391–396.
[10] S. Pitkäaho, S. Ojala, T. Maunula, A. Savimäki, T. Kinnunen, R.L. Keiski, Applied Catalysis B 102 (2011) 395–403.
[11] S. Pitkäaho, L. Matejova, S. Ojala, J. Gaalova, R.L. Keiski, Applied Catalysis B 113–114 (2012) 150–159.
[12] S. Pitkäaho, S. Ojala, T. Kinnunen, R. Silvonen, R.L. Keiski, Topics in Catalysis 54 (2011) 1257–1265.
[13] S. Lowel, J.E. Shields, M.A. Thomas, M. Thommes, Characterization of Porous Solids and Powders: Surface Area, Pore Size and Density, Springer, Dordrecht, 2010.
[14] X. Wu, S. Kawi, Energy and Environmental Science 3 (2010) 334–342.
[15] C. Zhang, H. He, K-i. Tanaka, Applied Catalysis B 65 (2006) 37–43.
[16] X.Y. Jiang, G.H. Ding, L.P. Lou, Y.X. Chen, X.M. Zheng, Journal of Molecular Catalysis A: Chemical 218 (2004) 187–195.
[17] J.Z. Shyu, W.H. Weber, H.S. Gandhi, Journal of Physical Chemistry 92 (1988) 4964–4970.
[18] J.Z. Shyu, K. Otto, Journal of Catalysis 115 (1989) 16–23.
[19] A.C.S.F. Santos, D. Damyanoca, G.N.R. Teixeira, L.V. Mattos, F.B. Noronha, F.B. Passos, J.M.C. Bueno, Applied Catalysis A 290 (2005) 123–132.
[20] A. Trovarelli, Catalysis Reviews 38 (1996) 439–520.
[21] L. Pino, A. Vita, M. Cordaro, V. Recupero, M.S. Hedge, Applied Catalysis A 243 (2003) 135–146.
[22] S. Damyanova, J.M.C. Bueno, Applied Catalysis A 253 (2003) 135–150.
[23] Z. Abbasi, M. Haghighi, E. Fatehifar, S. Saedy, Journal of Hazardous materials 186 (2011) 1445–1454.
[24] R. Ramírez-López, I. Elizalde-Martinez, L. Balderas-Tapia, Catalysis Today 150 (2010) 358–362.
[25] C.-B. Wang, C.-M. Ho, H.-K. Lin, H.-C. Chiu, Fuel 81 (2002) 1883–1887.
[26] W. Lin, Y.X. Zhu, N.Z. Wu, Y.C. Xie, I. Murwani, E. Kemnitz, Applied Catalysis B 50 (2004) 59–66.
[27] S. Parres-Esclapez, M.J. Illán-Gómez, C. Salinas-Martínez de Lecea, A. Bueno-López, Applied Catalysis B 96 (2010) 370–378.
[28] D. Martin, D. Duprez, Applied Catalysis A 131 (1995) 297–307.
[29] R. Burch, P.K. Loader, N.A. Cruise, Applied Catalysis A 147 (1996) 375–394.
[30] A. Guerrero-Ruiz, B. Bachiller-Baeza, P. Ferreira-Aparicio, I. Rodríguez-Ramos, Journal of Catalysis 171 (1997) 375–382.
[31] D. Techner, K. Matusek, Z. Paál, Journal of Catalysis 192 (2000) 335–343.
[32] R. Wang, H. Xu, X. Liu, Q. Ge, W. Li, Applied Catalysis A 305 (2006) 204–210.
[33] W.-Z. Weng, X.-Q. Pei, J.-M. Li, C.-R. Luo, Y. Liu, H.-Q. Lin, C.-J. Huang, H.-L. Wan, Catalysis Today 117 (2006) 53–61.
[34] I. Sarusi, K. Fodor, K. Baán, A. Oszkó, G. Pótári, A. Erdöhelyi, Catalysis Today 171 (2011) 132–139.
[35] G.C. Bond, S.F. Tahir, Applied Catalysis 71 (1991) 1–31.
[36] P. Van der Avert, B.M. Weckhuysen, Angewandte Chemie International Edition 41 (2002) 4730–4732.
[37] Ö. Orbay, S. Gao, B. Barbaris, E. Rupp, A.E. Sáez, R.G. Arnold, E.A. Betterton, Applied Catalysis B 79 (2008) 43–52.
[38] R.M. Heck, R.J. Farrauto, Catalytic Air Pollution Control: Commercial Technology, Van NostrandReinhold, New York, 1995.
[39] O. Koper, Y.X. Li, K.J. Klabunde, Chemistry of Materials 5 (1993) 500–506.
[40] B.M. Weckhuysen, G. Mestl, M.P. Rosynek, T.R. Krawietz, J.F. Haw, J.H. Lunsford, Journal of Physical Chemistry B 102 (1998) 3773–3778.
[41] B.M. Weckhuysen, M.P. Rosynek, J.H. Lunsford, Physical Chemistry Chemical Physics 1 (1999) 3157–3162.
[42] E.C. Rupp, E.A. Betterton, R.G. Arnold, A.E. Sáez, Catalysis Letters 132 (2009) 153–158.
[43] P. Van der Avert, S.G. Podkolzin, O. Manoilova, H. de Winne, B.M. Weckhuysen, Chemistry – A European Journal 10 (2004) 1637–1646.